Swelling of alginate gels in the presence of salts

Author: Patricia Masip Fernández, pmasipfe9@alumnes.ub.edu
Facultat de Física, Universitat de Barcelona, Diagonal 645, 08028 Barcelona, Spain.

Advisor: Alberto Fernández-Nieves

Abstract: Alginate gels are widely used in biomedical applications due to their biocompatibility and controllable swelling properties. While previous theories predict that ionic solvents degrade alginate gels through Ca^{2+} /Na^{+} exchange, breaking the Ca^{2+} cross-links and leading to degradation, our experiments with alginate capsules in solutions with varying concentrations of NaCl and $CaCl_2$ show a different behavior. The gel not only does not degrade, but with increasing concentrations of salts, it reaches a maximum size to then deswell, contradictory to the expectations. Modeling the gels as ionic allows explaining the observed behavior. This suggests that the swelling is mainly due to ionic effects rather than cross-link degradation.
Keywords: Alginate gels, Swelling, Donnan potential, Osmotic pressure.
SDGs: Health and well-being, Quality education, Industry, innovation and infrastructure.

I. INTRODUCTION

Alginate is an anionic polymer obtained from brown seaweed, which makes it a natural material widely used in biomedical applications due to its biocompatibility [1]. One example is its use in drug delivery capsules, done by Treefrog Therapeutics, our collaborator. These capsules are used to transport stem cells, which require specific salt concentrations and pH conditions. For this reason, analyzing the stability of the capsules under different conditions is important [2].

Polymers are formed by many monomers chemically linked, usually by covalent bonds. When the polymer chains are long enough, the bond angles become mostly uncorrelated, forming three-dimensional random coils. These polymers can be turned into gels when cross-links are added; these prevent polymer rearrangement. The cross-links can be physical, connecting the polymers through non-covalent bonds, or chemical, forming covalent bonds that make the connections permanent [3].

The presence of a solvent is essential for polymer gels since part of the solvent is absorbed and held within the polymer network. They are nevertheless solids even if mostly made of solvent [4]. The entropy of the polymer, together with the elastic stress from the cross-links, can be thought of in terms of osmotic pressure. It is the osmotic pressure difference between the inside and the outside of the gel what controls their swelling or deswelling [3].

Ionic gels contain fixed charged groups in their polymer structure. These charges lead to a Donnan potential, that causes an imbalance in ion distribution between the inside and outside of the gel, therefore, affecting the swelling behavior [5].

A. Alginate gels

The alginate polymer consists of β-D-mannuronic acid (M) and α-L-guluronic acid (G) monomer residues. Each polymeric block contains carboxylic groups (–COOH) that can dissociate depending on pH, creating fixed negative charges. This makes alginate an anionic gel when deprotonated. The electrostatic forces within the polymer network are strongly affected by the presence of ions from salts in the solvent [6].

Gelation occurs when divalent cations form ionic (physical) cross-links between two G-blocks from different polymer chains, creating the characteristic "egg-box" structure shown in Figure 1. This interaction is more favorable between G-blocks than M-blocks due to their specific spatial configuration, which facilitates the interaction with calcium ions. Calcium ions (Ca^{2+}) are the most commonly used for this purpose, as they are non-toxic [7].

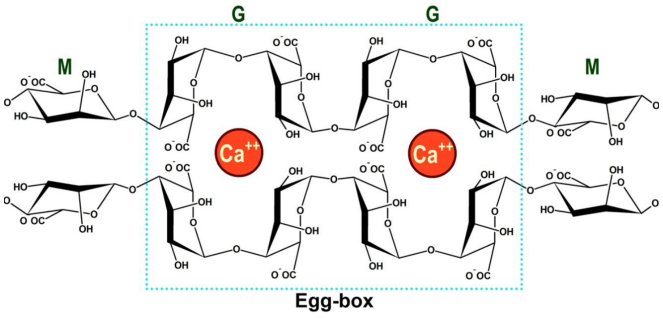

FIG. 1: Figure taken from [8] representing the "egg-box" structure in alginate gels ionically crosslinked with calcium ions.

According to the literature, Ca^{2+} cross-links are not completely stable, as calcium ions can be exchanged with monovalent cations like Na^{+} from the surrounding solu-

tion. This reduces the number of cross-links, causing the gel to swell and eventually degrade completely [1]. A high concentration of competing ions intensifies this effect, leading to more swelling and ending with the full dissolution of the gel.

B. Experimental deviations from theoretical predictions

When conducting experiments on gel size as a function of [NaCl] and [$CaCl_2$], we observe a behavior that is different from the one expected: while the gels initially swell (as predicted), they begin to deswell beyond certain [NaCl]. This contradicts the expectation of continuous swelling leading to complete dissolution. The observed deswelling suggests that at least some egg-box structures must remain formed rather than fully dissolving.

In the following sections, we describe our experimental work, discuss our results and propose an explanation that accounts for both the swelling and the deswelling of the gels.

II. METHODOLOGY

For our experiments, we use capsules produced by Treefrog Therapeutics. These capsules are made of alginate gel and are immersed in an aqueous solution, which acts as the solvent both inside and outside the gel network.

A. Experimental procedure

Prior to the experiments, all samples undergo dialysis to remove low molecular weight impurities. The capsules are enclosed in dialysis membranes with a molecular weight cut-off of 12-14 kDa and immersed in 6 L of ultrapure water. The external water is replaced three times to ensure efficient ion removal through diffusion. To monitor the solute removal, we measure the conductivity of the surrounding water; since dissolved ions from the original solution contribute to conductivity, stabilization of this value is an indicator of complete impurity removal.

Once the samples are cleaned, the capsules are immersed in different baths at varying concentrations of NaCl and $CaCl_2$ and in fixed pH conditions. All experiments are conducted at pH values above the pK_a of carboxylic acid in alginate, ~ 3.2 (derived in previous experiments conducted by the group), ensuring that most of the carboxylic groups are deprotonated and thus that the polymer network is charged.

Capsules are allowed to equilibrate in their respective solutions for 48 hours before the analysis. Due to their higher density compared to the surrounding medium, the capsules sediment, which allows them to be easily extracted with a pipette. To prevent deformation during imaging, samples are placed between two glass slides using a 1 mm thick melted paraffin frame.

All complete protocols of the procedure as well as the conductivity measurements are provided in Appendix A.

B. Imaging

To analyze the size variation of the capsules as a function of [NaCl] and [$CaCl_2$], we capture images from the Axio Observer Inverted microscope (Zeiss) with a 2.5x objective. Köhler illumination ensures homogeneous illumination in the field of view and eliminates the light source in the final image. This creates a grain-free and extended image, that enhances sample contrast [9].

Since capsules are relatively transparent, they are very hard to observe in normal microscope modes. This is why we use dark-field microscopy. This type of microscopy uses a spherically concave condenser to block unscattered light and only captures rays that have been scattered, reflected or refracted by the interfaces in the sample. This produces high-contrast images with bright edges against a dark background [10, 11].

C. Image processing

To analyze the size of the capsules, images are obtained using the ZEN software. The 2.5x objective of the microscope does not allow the entire suspension droplet to be captured in one single image. Therefore, we need to take overlapping pictures of the whole droplet. We use screen captures at 3-second intervals instead of downloading the images directly from the microscope software, as it is a faster process and the file size is notably reduced while having enough resolution for latter analysis. It is important that the scale bar provided by the software appears in the screenshots, as can be seen in the top and left of the image from Figure 2a, since it is used to obtain the pixel-to-micrometer conversion.

Each screenshot is cropped and stitched together using OpenCV algorithms that identify common patterns within all images provided, automatically stitching images. This process sometimes fails due to insufficient or repetitive features, so it has to be revised manually. An image of the entire stitched droplet can be observed in Figure 2b.

Capsules are detected using the Segment Anything Model (SAM), an open-source deep learning tool developed by Meta AI [12]. SAM has been trained over

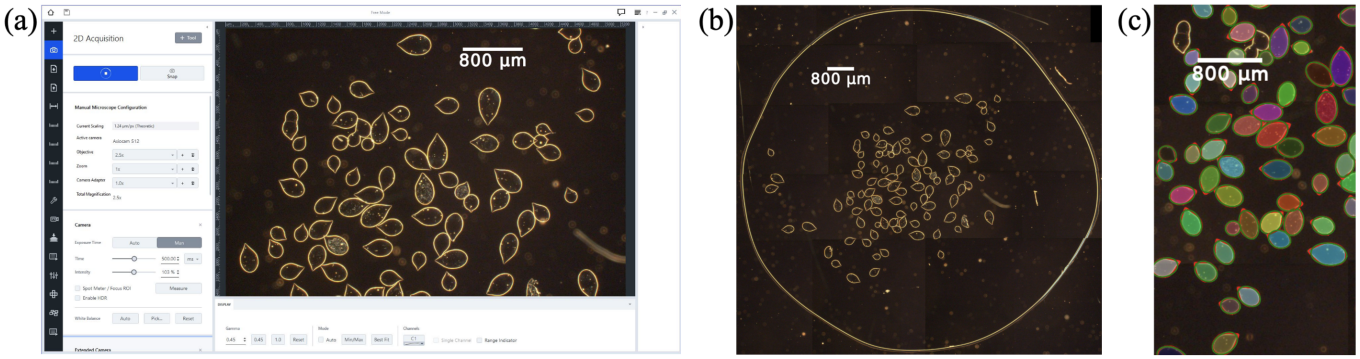

FIG. 2: Image processing steps. (a) Example screenshot taken from the ZEN microscope software. (b) Stitched image of the full suspension droplet after cropping and aligning all overlapping screenshots. (c) Section of the stitched image showing some of the detected capsules and the segmentation using the SAM model, different colors are used for each identified capsule, and the fitted ellipses, shown in green. The scale bars in all images correspond to 800 μm.

11 million images and 1 billion masks, providing a high success rate in detecting a wide variety of objects. When run on a GPU, SAM detects most capsules rapidly, though it needs to be manually revised since it also detects some additional objects.

To quantify the size of each capsule, we fit an ellipse to each detected object using the REGIONPROPS function from the Python library scikit-image, which returns the major and minor axes a and b, as well as the orientation of the fitted ellipse [13]. These values allow us to overlay the fitted ellipses on the original image, as can be seen in Figure 2c. We define the capsule diameter as $w = 2b$, averaging over all capsules. The ratio a/b is approximately constant, see Appendix B, except at the highest [NaCl] we probe. This guarantees that the gel is essentially in the linearly elastic regime.

We will then report on $\langle w \rangle$ and its standard error,

$$\text{Error}(\langle w \rangle) = \sqrt{\frac{\langle (\delta w)^2 \rangle}{N}} \tag{1}$$

where N is the number of detected capsules, and $\delta w = w - \langle w \rangle$, with $\langle \cdots \rangle$ the average over all capsules.

III. RESULTS

The experimental results are presented in Figure 3. The capsule diameter remains approximately constant at low [NaCl]. However, with further increase in the salt concentration, the gel begins to swell, reaching a maximum size before deswelling to values close to those observed initially. In these experiments $[CaCl_2] = 1$ mM.

Since both experimental batches were prepared under similar conditions, with the same $[CaCl_2]$ and a pH above the pK_a, they show very similar swelling behavior as [NaCl] increases.

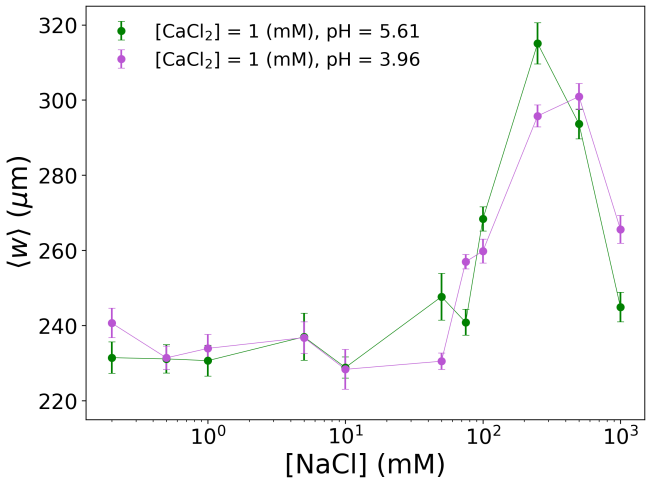

FIG. 3: Swelling behavior of alginate capsules as a function of NaCl concentration at fixed $CaCl_2$ concentration and pH. Swelling is quantified through mean capsule diameter with its standard error.

This behavior cannot be explained only by assuming that the gel dissolves due to the release of Ca^{2+} ions. Therefore, we propose an alternative interpretation based on treating alginate gels as regular ionic gels, where fixed charges originating from deprotonated carboxylic groups generate a Donnan potential. In this situation, swelling is mainly caused by the osmotic pressure difference between mobile ions inside and outside the gel network, which we consider to be the dominant contribution.

To understand this behavior, we follow the theoretical model developed by Tanaka [14] and later extended by Fernández-Nieves [15].

A. The model

To interpret the swelling behavior observed experimentally, we model the alginate capsule as a charged ionic gel in equilibrium with the surrounding ionic solution.

We assume that the gel allows the entry of mobile ions while retaining fixed charges originating from dissociated carboxylic acid groups. Therefore, when a free ion from the solvent enters the gel, it feels an energy $E_1 = U$ that corresponds to the Donnan potential. This potential results from a balance between electrostatic forces that attract counter-ions and repel co-ions due to the fixed negative charges; and entropic effects, that favor uniform ion distribution to maximize entropy. Therefore, it depends on the relative volume available to ions and the ratio of internal and external ion concentrations.

The carboxylic groups dissociate as $COOH \rightleftarrows COO^- + H^+$ with a dissociation constant $K_a = \frac{n_{COO^-} n_{H^+}}{n_{COOH}}$ where n_{COOH} and n_{COO^-} are the concentrations of the undissociated and dissociated carboxylic groups, respectively. Therefore, the total concentration of carboxylic groups in the polymer, whether dissociated or not, is defined as $\rho = n_{COOH} + n_{COO}$; this corresponds to the total number of monomers present in the polymer.

The gel is immersed in a bath containing mobile ions Na^+, Cl^-, H^+, OH^-, and Ca^{2+}. The equilibrium concentration of each ionic species inside the gel can be defined using Boltzmann statistics:

$$n_i = n_i^* e^{-\frac{z_i e U}{k_B T}} = n_i^* \lambda^{z_i} \tag{2}$$

where U is de Donnan potential, $n_i = \frac{N_i}{V_i}$ is the concentration of ion i inside the gel, with N_i the number of ions inside the gel, n_i^* is the concentration of ion i outside the gel, z_i the valence of the ion i, e the elementary charge and k_B the Boltzmann constant. The Donnan ratio, λ, is introduced to simplify the expression.

Since the gel must remain electrically neutral, the concentrations of all charged species inside the gel must satisfy the electroneutrality condition:

$$2n_{Ca} + n_{Na} + n_H = n_{Cl} + n_{OH} + n_{COO} \tag{3}$$

The variables that can be controlled experimentally are the concentrations in the solvent (that are assumed fully ionized). By substituting the expressions from Equation 2 into Equation 3, we obtain a nonlinear polynomial equation that can be solved numerically to find the Donnan ratio λ, and then, determine the internal ion concentrations through Equation 2. We solve it numerically using the ROOTS function from the NumPy Python library [16].

Once the ion concentrations inside the gel are known, the osmotic pressure difference between the inside and outside of the gel can be calculated assuming the ions behave as an ideal gas:

$$\Delta\pi = N_A k_B T \sum_i (n_i - n_i^*) \tag{4}$$

where N_A is Avogadro's number, and the sum goes over all mobile ionic species.

The detailed calculations of the model are provided in Appendix C.

Using the model described above, we have numerically solved for the ionic osmotic pressure difference for the case of [$CaCl_2$]= 1 mM and $pH = 5.6$. The values used for the dissociation constant and the fixed charge density have been choosen based on the results of previous experiments conducted by the group; they are $pK_a = 3.2$ and $\rho = 0.8$ M. Ensuring that the conditions are as similar as possible to the experimental ones, the results for $\Delta\pi$ as a function of [NaCl] are shown in Figure 4.

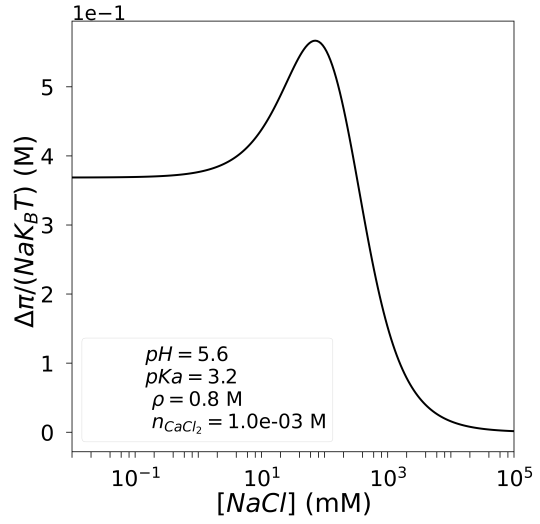

FIG. 4: Normalized osmotic pressure difference due to the ions as a function of NaCl concentration. The parameters in the calculation are: $pH = 5.6$ in the solvent, $pK_a = 3.2$, $\rho = 0.8$ M and [$CaCl_2$]= 1 mM.

Although the experimental and theoretical results represent different physical quantities (capsule size in Figure 3 and osmotic pressure in Figure 4) the model correctly matches the trends observed in the experiments. Some discrepancies may result from the limited precission in the pK_a and ρ, which were chosen based on what best matched the behavior observed in previous experiments conducted by the group.

At low salt concentrations, the osmotic pressure remains relatively low and constant, resulting in very little volume change. In this region, Ca^{2+} is the dominant

counterion inside the gel. Since Ca^{2+} feels a higher attraction strength compared to H^+, higher quantites of this ion will be present in the gel ($n_{Ca} >> n_H$), this creates a stable situation in which the osmotic pressure remains relatively constant.

As the [NaCl] increases, Ca^{2+} ions are replaced by two Na^+ ions to maintain electroneutrality. This raises the total ionic concentration inside the gel. When both concentrations are comparable, the gel starts to swell due to the increase of ions inside the gel, which causes a difference between the inside and the outside that creates an osmotic pressure.

Beyond a critical [NaCl], Cl^- ions start to enter the gel due to entropic effects. This increase in anion concentration inside the gel causes the Donnan potential to reduce, which makes the capsules deswell with a similar trend to the initial swelling region.

When the [NaCl] increases enough, the Donnan potential tends to zero, and the ionic concentrations inside and outside the gel equilibrate.

IV. CONCLUSIONS

These results suggest that the proposed theoretical model is consistent with the physics that cause the observed swelling behavior. We conclude that the swelling and deswelling of alginate gels are not primarily due to the breakdown of "egg-box" structures. Instead, the gels behave as ionic gels, with volume changes due to electrostatic interactions and the resulting osmotic pressure differences between the gel interior and the external solution.

This contrasts with previous knowledge on the behavior of alginate gels and provides new information that can be relevant for all types of industries that use these materials. Understanding better how they swell in different salt conditions helps us predict their durability and how their structure varies. This knowledge is particularly relevant for pharmaceutical applications, where the control of gel behavior is essential for drug delivery applications.

Acknowledgments

I would like to express my sincere gratitude to my advisor, Alberto Fernández-Nieves, for all the support and trust he has placed in me through this project. I also want to thank Guillaume Briand for sharing so much knowledge, providing constant support, and making the time spent doing experiments and analysis so enjoyable. I also am grateful to Treefrog Therapeutics for supporting this research. Finally, I want to express a very strong appreciation to my friends for their encouragement and support, not only during this project, but throughout the entire bachelor's degree.

[1] Lee, K.Y. and Mooney, D.J. "Alginate: properties and biomedical applications," *Progress in Polymer Science*, vol. 37, no. 1, pp. 106–126, 2012.
[2] Treefrog Therapeutics. *https://treefrog.fr/* [Accessed June 2025].
[3] Dimitriyev, M. S. *et al.* "Swelling thermodynamics and phase transitions of polymer gels", *Nano Futures*, vol. 3, 042001, 2019.
[4] Banerjee, S. and Tyagi, A. K. "Soft Materials — Properties and Applications," in *Functional Materials: Preparation, Processing and Applications*, Chapter 1.5.6: Polymer Gels. Elsevier, 2012.
[5] Fernández-Nieves, A. *et al. Microgel Suspensions: Fundamentals and Applications*, Wiley-VCH, 2011.
[6] Donati, I. and Paoletti, S. "Material Properties of Alginates," in *Alginates: Biology and Applications*, vol. 13, pp. 1–53, Springer, 2009.
[7] Ching, S. H. *et al.* "Alginate gel particles: A review of production techniques and physical properties," *Critical Reviews in Food Science and Nutrition*, vol. 57, no. 6, pp. 1133–1152, 2017.
[8] Lee, H-R. et al. "Immobilization of planktonic algal spores by inkjet printing". *Scientific Reports*, 2019. Nature Research.
[9] M. W. Davidson. "Configuring a Microscope for Köhler Illumination," ZEISS Microscopy Campus. `https://zeiss-campus.magnet.fsu.edu/articles/basics/kohler.html` [Accessed June 2025].
[10] A. De Grand. "What is Darkfield Microscopy?" Olympus Life Science, 2020. `https://www.olympus-lifescience.com/en/discovery/what-is-darkfield-microscopy/` [Accessed June 2025].
[11] Microbe Online. "Dark Field Microscopy." `https://microbeonline.com/dark-field-microscopy/` [Accessed June 2025].
[12] Kirillov, A. et al. "Segment Anything,", 2023.
[13] Scikit-Image Documentation. "Regionprops." `https://scikit-image.org/docs/0.24.x/auto_examples/segmentation/plot_regionprops.html` [Accessed June 2025].
[14] Ricka, J. and Tanaka, T. "Swelling of ionic gels: quantitative performance of the Donnan theory", *Macromolecules*, vol. 17, no. 12, pp. 2916–2921, 1984.
[15] Fernández-Nieves, A. *et al.* "Salt effects over the swelling of ionized mesoscopic gels", *The Journal of Chemical Physics*, vol. 115, no. 16, pp. 7644–7649, 2001.
[16] NumPy Documentation. "numpy.roots" `https://numpy.org/doc/2.2/reference/generated/numpy.roots.html` [Accessed June 2025].

Expansió dels gels d'alginat per absorció de solvent en presència de sals

Author: Patricia Masip Fernández, pmasipfe9@alumnes.ub.edu
Facultat de Física, Universitat de Barcelona, Diagonal 645, 08028 Barcelona, Spain.

Advisor: Alberto Fernández-Nieves

Resum: Els gels d'alginat s'utilitzen sovint en aplicacions biomèdiques gràcies a la seva biocompatibilitat i a les seves propietats d'expansió controlable per absorció de solvent. Tot i que teories prèvies prediuen que les solucions iòniques degraden els gels d'alginat mitjançant l'intercanvi de Ca^{2+} i Na^{+}, afeblint els encreuaments de Ca^{2+} i provocant la degradació del gel, els experiments duts a terme amb càpsules d'alginat en solucions amb concentracions variables de NaCl i $CaCl_2$ mostren un comportament diferent. El gel no només no es degrada, sinó que, amb l'augment de la concentració de sals, arriba a una mida màxima i després decreix, contradient les expectatives. Modelitzar els gels com a gels iònics permet explicar aquest comportament observat. Això suggereix que els canvis de volum es deuen principalment a efectes iònics i no a la degradació dels encreuaments de Ca^{2+}.
Paraules clau: Gels d'alginat, Expansió per absorció de solvent, Potencial de Donnan, Pressió osmòtica.
ODSs: Salut i benestar, Educació de qualitat, Indústria, innovació, infraestructures.

Objectius de Desenvolupament Sostenible (ODSs o SDGs)

1. Fi de la es desigualtats		10. Reducció de les desigualtats	
2. Fam zero		11. Ciutats i comunitats sostenibles	
3. Salut i benestar	X	12. Consum i producció responsables	
4. Educació de qualitat	X	13. Acció climàtica	
5. Igualtat de gènere		14. Vida submarina	
6. Aigua neta i sanejament		15. Vida terrestre	
7. Energia neta i sostenible		16. Pau, justícia i institucions sòlides	
8. Treball digne i creixement econòmic		17. Aliança pels objectius	
9. Indústria, innovació, infraestructures	X		

Aquest TFG, part del grau de Física de la Universitat de Barcelona, es relaciona amb l'ODS 3, i en particular amb la fita 3.B, ja que els resultats obtinguts tenen una potencial aplicació en tractaments biomèdics. També es relaciona amb l'ODS 4, concretament amb la fita 4.3, perquè contribueix a l'educació en l'àmbit universitari. Finalment, amb l'ODS 9, fita 9.5, ja que promou la investigació científica.

Appendix A: EXPERIMENTS

1. Dialysis protocol

- We grab 10 mL of the sample containing the capsules provided by Treefrog Therapeutics.
- We use 10 cm of dialysis membrane with a molecular weight cut-off of 12-14 kDa.
- Before use, the dialysis membranes have to be cleaned to remove surface impurities. This is done by boiling them three times in ultrapure water, replacing the water between each boil.
- We fill the membranes with the sample, seal them with clips and immerse them in 6 L of ultrapure water.
- We replace the external water twice to ensure the complete removal of the low molecular weight impurities.
- The conductivity is measured after each replacement.

The results of the conductivity measurements are shown in Table I.

TABLE I: Date, conductivity, and temperature for dialysis experiment.

Date	Conductivity (μs/cm) 1	Temperature (°C)
17/10/2024	3.50	23.6
21/10/2024	13.62	25.0
29/10/2024	2.30	22.1

2. Bath preparation

The experiments require the preparation of baths with different pH and salt concentrations, in which the alginate capsules are immersed.

To begin, we prepare two bottles of the following concentrations:

- NaCl at a concentration $[\mathrm{NaCl}]_0 = 1$ M.
- $CaCl_2$ at a concentration $[\mathrm{CaCl_2}]_0 = 100$ mM.

These solutions were made using solid NaCl and $CaCl_2{\cdot}2H_2O$ powder. The required mass used in each case is calculated using the following relations:

- Number of moles:

$$n(X) = \frac{m(X)}{M(X)} \tag{A1}$$

where $m(X)$ is the mass and $M(X)$ is the molar mass.

- Concentration:

$$[X] = \frac{n(X)}{V} \tag{A2}$$

where V is the volume of solution to prepare.

Therefore, the required mass is $m(X) = V \cdot [X] \cdot M[X]$.

Once the bottles are prepared, we can make each bath using mass conservation:

$$V_0 = \frac{[X] \cdot V}{X_0} \tag{A3}$$

where subindex 0 refers to the original bottle and the terms without subindex refer to the bath we want to prepare.

To control the pH, we used a liquid made of 37% HCl. In this case, it is also necessary to take into account the relative density of the solution, defined as $d = \frac{\rho(X)}{\rho(H_2O)}$. The mass is calculated as $m(X) = \rho(X) \cdot V$. This allows determining the volume of the HCl solution required to prepare each bath at a certain pH.

We set the total volume of the baths at $V_{tot} = 3$ mL. Each bath is prepared by mixing the calculated volumes of each solution and diluting them to the final volume with ultrapure water. To ensure the complete and homogeneous dissolution of the salts, we use magnetic stirring.

For this work, we have prepared baths of the same $[CaCl_2] = 1$ mM and [NaCl] that range from 0.1 mM to 1000 mM. For these conditions, we have made one batch at pH = 5.61 and another batch at pH = 3.96. In both cases, above the $pK_a \approx 3.2$ of the carboxylic groups in alginate, ensuring that most of these groups are deprotonated during the experiment.

3. Capsule deposition for imaging

To extract the capsules from each bath, we need a pipette with an opening wide enough to allow the capsules to pass through without damage. Since we are working with very small volumes, the pipette tips were manually cut to obtain the desired diameter.

The capsules are then placed between two glass slides. To prevent their deformation during imaging, a 1 mm thick frame of melted parafilm was made around the lower slide, as shown in Figure 5.

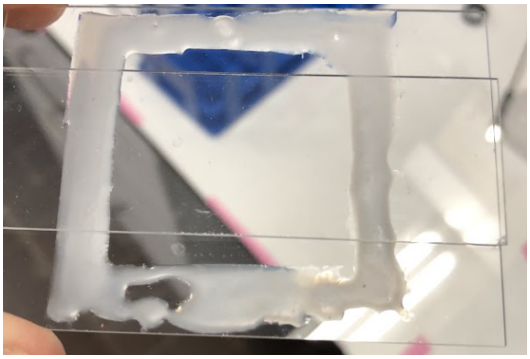

FIG. 5: Structure made of two glass slides and melted parafilm to prevent capsule deformation.

Appendix B: Linearly elastic regime

To verify that the capsules remain in the elastic regime, we analyze the relationship between the major axis a and minor axis b of the fitted ellipses. Specifically, we plot the ratio $\langle b\rangle/\langle a\rangle$ as a function of [NaCl]. The results can be seen in Figure 6, corresponding to the conditions $[CaCl_2] = 1$ mM and pH = 5.61.

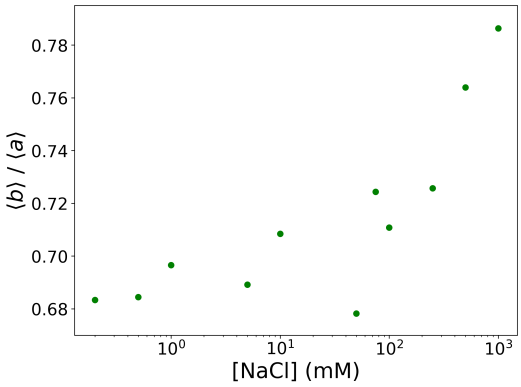

FIG. 6: Ratio between the average minor and major axes, $\langle b\rangle/\langle a\rangle$, as a function of [NaCl] for $[CaCl_2] = 1$ mM and pH = 5.61.

It is noticeable how the ratio remains mostly constant, especially at low [NaCl], which suggests that the capsules are in the linearly elastic regime.

Appendix C: Model calculation

To describe the ion distribution inside the gel, we use Boltzmann statistics to relate the concentrations of each ion species inside and outside the gel:

$$n_i = n_i^* e^{-\frac{z_i e U}{k_B T}} = n_i^* \lambda^{z_i} \tag{C1}$$

The total concentration of carboxylic groups (total number of monomers) is given by $\rho = n_{\mathrm{COOH}} + n_{\mathrm{COO}}$ and the dissociation constant is $K_a = \frac{n_{\mathrm{COO^-}} n_{\mathrm{H^+}}}{n_{\mathrm{COOH}}}$. We can express the concentration of n_{COO} and n_{COOH} as:

$$n_{COO} = \frac{\rho}{\frac{n_H}{K_a} + 1} \tag{C2}$$

$$n_{COOH} = \frac{\rho}{\frac{K_a}{n_H} + 1} \tag{C3}$$

To maintain electroneutrality inside the gel, the sum of positive and negative charges must balance. Substituting the expression for n_{COO}, we have:

$$2n_{\mathrm{Ca}} + n_{\mathrm{Na}} + n_{\mathrm{H}} = n_{\mathrm{Cl}} + n_{\mathrm{OH}} + \frac{\rho}{\frac{n_H}{K_a} + 1} \tag{C4}$$

$$\left(1 + \frac{n_H}{K_a}\right)(2n_{\mathrm{Ca}}+n_{\mathrm{Na}}+n_{\mathrm{H}}) = \left(1 + \frac{n_H}{K_a}\right)(n_{\mathrm{Cl}}+n_{\mathrm{OH}})+\rho \tag{C5}$$

$$\begin{aligned} &2n_{\mathrm{Ca}} + n_{\mathrm{Na}} + n_{\mathrm{H}} + \frac{n_H}{K_a}(2n_{\mathrm{Ca}} + n_{\mathrm{Na}} + n_{\mathrm{H}}) \\ &= n_{\mathrm{Cl}} + n_{\mathrm{OH}} + \frac{n_H}{K_a}(n_{\mathrm{Cl}} + n_{\mathrm{OH}}) + \rho \end{aligned} \tag{C6}$$

If we replace the inside concentrations with the Boltzmann relation, and group terms with respect to the power of λ, we obtain the following:

$$\begin{aligned} &2n_c^* n_{\mathrm{Cl}}^* \lambda^2 + n_{\mathrm{H}}^* \lambda + \frac{n_{\mathrm{H}}^*}{K_a}(2n_c^* n_{\mathrm{Cl}}^* \lambda^2 + n_{\mathrm{H}}^* \lambda + n_{\mathrm{Na}}^* \lambda) \\ &= (n_{\mathrm{OH}}^* \lambda^{-1} + n_{\mathrm{Cl}}^* \lambda^{-1}) + \frac{n_{\mathrm{H}}^*}{K_a}(n_{\mathrm{OH}}^* \lambda^{-1} + n_{\mathrm{Cl}}^* \lambda^{-1}) + \rho \end{aligned} \tag{C7}$$

$$\begin{aligned} \lambda^4 &+ \frac{K_a}{2n_c^* n_{\mathrm{H}}^*}\left(2n_c^* + \frac{n_{\mathrm{H}}^*}{K_a}(n_{\mathrm{H}}^* + n_{\mathrm{Na}}^*)\right)\lambda^3 \\ &+ \frac{K_a}{2n_c^* n_{\mathrm{H}}^*}(n_{\mathrm{H}}^* + n_{\mathrm{Na}}^*)\lambda^2 \\ &- \frac{K_a}{2n_c^* n_{\mathrm{H}}^*}\left(\frac{n_{\mathrm{H}}^*}{K_a}(n_{\mathrm{OH}}^* + n_{\mathrm{Cl}}^*) + \rho\right)\lambda \\ &- \frac{K_a}{2n_c^* n_{\mathrm{H}}^*}(n_{\mathrm{OH}}^* + n_{\mathrm{Cl}}^*) = 0 \end{aligned} \tag{C8}$$

This expression can be solved numerically for λ using the ROOTS function from the NumPy Python library.

To solve it, we have to take into account some considerations:

- $\mathrm{pH} = -\log(n_{\mathrm{H}}^*)$, so $n_{\mathrm{H}}^* = 10^{-\mathrm{pH}}$.
- $\mathrm{p}K_a = \log(K_a)$.
- $\mathrm{pOH} = -\log(n_{\mathrm{OH}}^*)$.

- We impose the concentrations of [NaCl] and [$CaCl_2$] outside. Therefore, $n^*_{\text{Na}} = n_1$, $n^*_{\text{Ca}} = n_2$ and $n^*_{\text{Cl}} = n_1 + 2n_2$.
- Since the ionizable groups are negatively charged, the counterions (positive ions) are more strongly attracted to the gel. This implies that $\lambda^{z_i} > 1$ for $z_i > 0$, so that $\lambda > 1$.

Once the Donnan ratio, λ is determined, we can compute the inside concentrations of all ionic species.

The osmotic pressure difference between the inside and the outside of the gel is given by:

$$\Delta\pi_i = N_A k_B T \sum_i (n_i - n_i^*), \tag{C9}$$

where N_A is Avogadro's number, and the sum goes over all mobile ionic species.